Dystrophin and utrophin have distinct effects on the structural dynamics of actin

Ewa Prochniewicz, Davin Henderson, James M. Ervasti, and David D. Thomas[1]

Department of Biochemistry, Molecular Biology, and Biophysics, University of Minnesota, Minneapolis, MN 55455

Edited by James A. Spudich, Stanford University School of Medicine, Stanford, CA, and approved March 24, 2009 (received for review November 25, 2008)

We have used time-resolved spectroscopy to investigate the structural dynamics of actin interaction with dystrophin and utrophin in relationship to the pathology of muscular dystrophy. Dystrophin and utrophin bind actin in vitro with similar affinities, but the molecular contacts of these two proteins with actin are different. It has been hypothesized that the presence of two low-affinity actin-binding sites in dystrophin allows more elastic response of the actin–dystrophin–sarcolemma linkage to muscle stretches, compared with utrophin, which binds via one contiguous actin-binding domain. We have directly tested this hypothesis by determining the effects of dystrophin and utrophin on the microsecond rotational dynamics of a phosphorescent dye attached to C374 on actin, as detected by transient phosphorescence anisotropy (TPA). Binding of dystrophin or utrophin to actin resulted in significant changes in the TPA decay, increasing the final anisotropy (restricting the rotational amplitude) and decreasing the rotational correlation times (increasing the rotational rates and the torsional flexibility). This paradoxical combination of effects on actin dynamics (decreased amplitude but increased rate) has not been observed for other actin-binding proteins. Thus, when dystrophin or utrophin binds, actin becomes less like cast iron (strong but brittle) and more like steel (stronger and more resilient). At low levels of saturation, the binding of dystrophin and utrophin has similar effects, but at higher levels, utrophin caused much greater restrictions in amplitude and increases in rate. The effects of dystrophin and utrophin on actin dynamics provide molecular insight into the pathology of muscular dystrophy.

muscular dystrophy | spectroscopy | flexibility | phosphorescence

Dystrophin and utrophin are large cytoskeletal proteins. In skeletal muscle, dystrophin is located within a cytoskeletal lattice termed the costamere, which is proposed to transmit the contractile force from the myofibrils to the extracellular matrix and adjacent muscle fibers (1, 2). The absence of dystrophin in patients with Duchenne muscular dystrophy is associated with defects in sarcolemmal elasticity (3) and integrity (4). It has been demonstrated that dystrophin provides a direct mechanical link between costameric actin filaments, comprising γ-actin and the sarcolemma (5), which may be critical for stabilization of the sarcolemma against stress developed during muscle contraction (4).

Utrophin expression is developmentally regulated: it is distributed throughout the sarcolemma of fetal and regenerating muscle but is down-regulated in normal adult muscle. Because utrophin binds to the same proteins as dystrophin, it has been proposed that utrophin performs the same role in developing muscle as dystrophin in mature muscle (6). In support of this hypothesis, transgenic overexpression of utrophin in dystrophin-deficient *mdx* mice prevents development of muscular dystrophy (7), most probably by rescuing the defective mechanical linkage between costameric actin and the sarcolemma (8).

Although in vivo studies indicate that dystrophin and utrophin play similar physiological roles, in vitro studies suggest that they do not act through the same biochemical pathways. Both dystrophin and utrophin bind to actin with similar affinities, and both stabilize actin filaments against depolymerization (9). However, dystrophin and utrophin differ in their effects on the extent of lateral association with actin and in the ionic strength dependence of actin binding, and they do not compete for the same binding sites on the actin filament (9). The two proteins also have similarities and differences in the structures of their actin-binding domains. Both contain N-terminal tandem calponin homology actin-binding domains. In utrophin, the whole actin-binding domain is completed by the first 10 spectrin-like repeats, whereas in dystrophin the first 10 spectrin-like repeats do not bind actin; there is a second actin-binding domain involving spectrin repeats 11–17 (10). Structural analysis of the molecular contacts between dystrophin and utrophin with actin has been limited to the contacts with their N-terminal domains, Dys246 and Ut261, respectively. Docking of crystal structures of each domain to the electron densities of its complex with actin indicated interaction with three regions of actin: the DNase-binding loop in subdomain 2, the C terminus in subdomain 1, and the helix in subdomain 4 (11), but the difference in the size and shape of bound Dys246 and Ut261 suggested that Dys246 forms more extensive contacts, which are proposed to be better suited for stabilization of the sarcolemma during muscle contraction (12).

Because utrophin has the potential to rescue the dystrophic phenotype, design of therapies requires more studies comparing the mechanisms of molecular interactions of utrophin and dystrophin, particularly of their effects on actin structure and dynamics. It has been proposed that the presence of two low-affinity actin-binding sites in dystrophin allows for a more elastic response of the actin–dystrophin–sarcolemma linkage to muscle stretches, compared with binding of utrophin via one contiguous actin-binding domain (9). The present study is designed to test this hypothesis directly by comparing the effects of the two proteins on the structural dynamics of actin. Our previous studies established transient phosphorescence anisotropy (TPA) as a powerful method for analyzing the effects of diverse actin-binding proteins on the microsecond rotational dynamics within the actin filament (13–17). We showed that changes in actin dynamics are specific to the interacting protein (14, 15) and to the functional properties of the actomyosin complex (16, 17). The present study applies TPA to test the hypothesis that the molecular mechanism of function of these two proteins involves specific effects on the dynamic properties of actin.

Results

Binding of Utrophin and Dystrophin to ErIA-Actin. Binding of full-length dystrophin and utrophin to erythrosin iodoacetamide-labeled actin (ErIA-actin) was determined under the same experimental conditions (6 μM actin, varying the concentration of the added protein) as used with unlabeled actin (9) (Fig. 1). The best fits to Eq. **1** gave $B_{max} = 0.064 \pm 0.015$ and $K_d = 0.95 \pm$

Author contributions: E.P. and D.H. performed research; and J.M.E. and D.D.T. wrote the paper.

The authors declare no conflict of interest.

This article is a PNAS Direct Submission.

[1]To whom correspondence should be addressed. E-mail: ddt@umn.edu.

www.pnas.org/cgi/doi/10.1073/pnas.0812007106

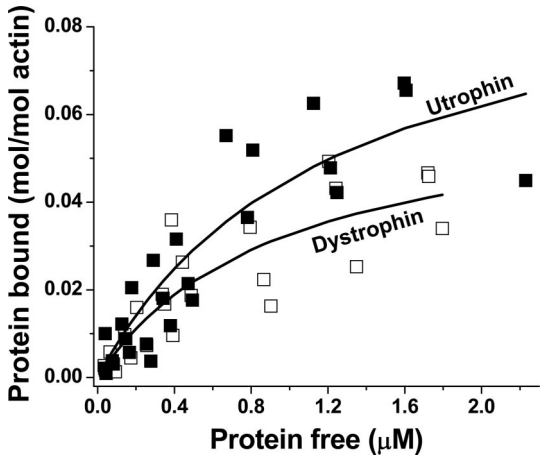

Fig. 1. Binding of dystrophin (open symbols) and utrophin (filled symbols) to ErIA F-actin. Solid lines represent best fits to Eq. **1**.

0.46 μM for dystrophin; $B_{max} = 0.10 \pm 0.02$ and $K_d = 1.21 \pm 0.50$ μM for utrophin. These values, which are similar to those reported for unlabeled actin binding to dystrophin (9, 18) or utrophin (8, 9), are used below to obtain values for the fraction of actin protomers that are bound to dystrophin or utrophin, so the effects of the two proteins can be compared quantitatively.

Because ErIA-actin used in binding assays and spectroscopic experiments was stabilized with phalloidin, we performed control experiments testing the effect of phalloidin on actin binding. Because of instability of phalloidin-free ErIA-actin (17, 19), these experiments were performed by using unlabeled actin. Twelve micromolar phalloidin had no effect on the extent of binding 0.3 μM utrophin to 6 μM actin. We conclude that actin-bound phalloidin has no effect on binding to utrophin and that reported inhibitory effects of phalloidin on interaction with the N terminus of utrophin (20) are not applicable to the interaction with the full-length protein.

Effects of Dystrophin and Utrophin on TPA of Actin. Both dystrophin and utrophin decrease the amplitude of the actin microsecond TPA decay, implying restriction of rotational dynamics, but the effects of utrophin are much greater than those of dystrophin (Fig. 2).

TPA experiments were performed over a wide range of added utrophin or dystrophin and then analyzed in detail (13) by fitting the data with Eq. **2** and plotting the resulting amplitudes and correlation times as a function of the fraction of actin protomers

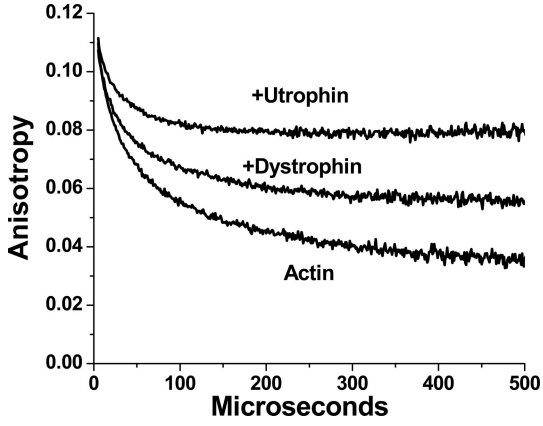

Fig. 2. Effect of 1.5 μM dystrophin and 2 μM utrophin on TPA decay of 1 μM ErIA-actin.

bound to dystrophin or utrophin (Fig. 3). This fraction of bound actin was calculated as (dystrophin or utrophin bound, mol/mol of actin)/B_{max}, assuming $B_{max} = 0.064$ for dystrophin and 0.10 for utrophin, as determined in Fig. 1. The most dramatic change was an increase in final anisotropy (r_∞, Fig. 3*A*), indicating decreased amplitude of microsecond flexibility, because of both bending and twisting of the actin filament (16, 17) (Fig. 4). At low concentrations of added proteins, where <10% of actin protomers are bound, dystrophin and utrophin had similar effects. However, as the fraction of bound actin increased, the increase in anisotropy in the presence of utrophin was substantially greater than in the presence of dystrophin, indicating that utrophin is more effective in restricting the amplitude of the actin microsecond rotational dynamics. When modeled as an isotropic filament bending motion (Eq. **4**), the amplitude of flexibility (defined as the half-cone angle) was 57° for actin alone, 36° for saturated dystrophin-actin, and 29° for saturated utrophin-actin. Dystrophin and utrophin also had different effects on the initial anisotropy of actin (Fig. 3*B*), which reflects submicrosecond flexibility within the actin protomer (13): utrophin increased this parameter, indicating decreased amplitude of submicrosecond dynamics, from 35° to 33° (Eq. **3**), whereas dystrophin had no significant effect.

TPA analysis (13) resolves two modes of actin rotational dynamics in the microsecond time range (Eq. **2** and Fig. 3). A slow mode, probably dominated by bending motions, is characterized by a correlation time ϕ_1 (inversely related to the rate of rotation) ≈200 μs. A fast mode, probably dominated by twisting motions, is characterized by ϕ_2 that is nearly 10 times shorter. Fig. 3*C* shows that bound dystrophin and utrophin decreased both rotational correlation times, implying increased rates of bending and twisting, and the corresponding amplitudes r_1 and r_2 (Fig. 3*D*), implying restricted angular amplitudes of bending and twisting. In both cases, it is striking that the rates of motion increase while the angular amplitudes decrease. Again, the effects of utrophin on all four of these parameters were much greater than those of dystrophin. The most striking effects were a 4-fold decrease in the long correlation time (ϕ_1) caused by utrophin while dystrophin decreased ϕ_1 by less than a factor of 2 (Fig. 3*C*), and a 3-fold decrease in the amplitude r_2 of the fast motion caused by utrophin while dystrophin decreased r_2 by less than a factor of 2 (Fig. 3*D*).

The effect of dystrophin and utrophin on TPA decay was further analyzed in terms of a specific model of actin rotational dynamics, in which actin is a homogeneous elastic rod undergoing intrafilament torsional twisting motions (Eq. **5**). We have shown that this model fits actin TPA decays well (13), with substantial effects on actin torsional rigidity caused by actin-binding proteins such as gelsolin (14), myosin (16, 21), and cofilin (15). To accommodate the basic assumption of the model that actin is a homogeneous elastic rod, the effects of dystrophin and utrophin on the torsional motions in actin were analyzed under conditions where ≈60% of actin protomers were bound (Fig. 1). The results showed that dystrophin and utrophin decrease the torsional rigidity (increase the torsional elasticity) of actin by 26 ± 8% and 78 ± 3%, respectively. Once again, utrophin is much more effective than dystrophin in affecting actin dynamics.

The phosphorescence intensity decays of actin in the presence of saturating dystrophin and utrophin showed that the lifetimes and amplitudes of the actin-bound phosphorescent probe were not significantly affected by either protein (Fig. 5). We conclude that bound proteins had negligible effects on the local environment of the probe, so TPA effects were caused by changes in actin filament rotational dynamics.

Utrophin Does Not Affect Filament Interactions. We have interpreted TPA data in terms of dynamics within isolated actin filaments, but it is important to consider actin filament interac-

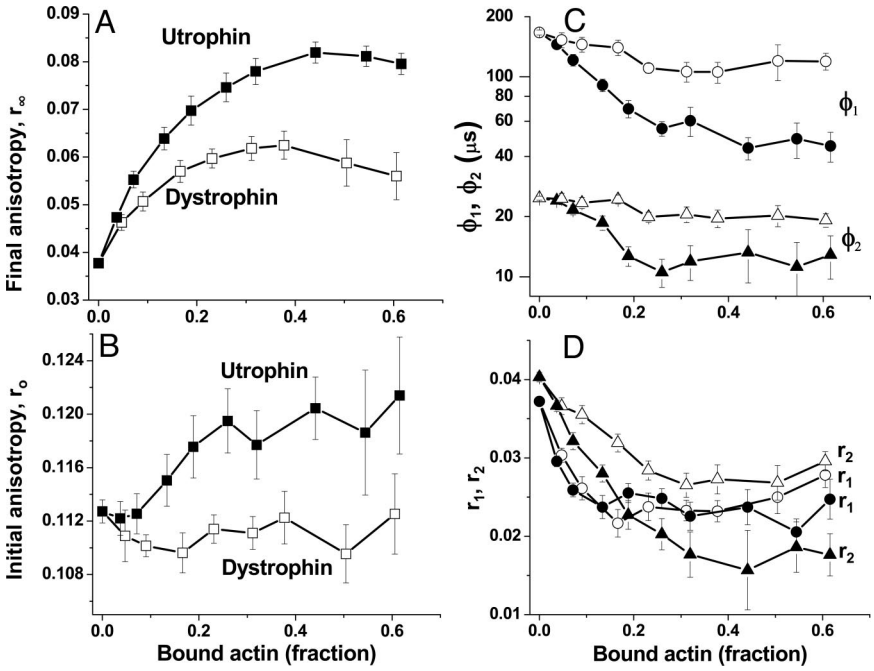

Fig. 3. Effect of dystrophin (open symbols) and utrophin (filled symbols) binding on the TPA of actin, as indicated by parameters derived from fitting the data with Eq. **2**. (*A*) Final anisotropy (r_∞). (*B*) Initial anisotropy (r_0). (*C*) Correlation times. (*D*) Amplitudes. (*C* and *D*) Circles and Triangles correspond to the slower (ϕ_1, r_1) and faster (ϕ_2, r_2) motions, respectively.

tions, which could restrict actin dynamics. This is of special concern for utrophin, which induces much greater restriction of the amplitude of the actin rotational dynamics in the presence of utrophin than dystrophin (Figs. 2 and 3), suggesting that utrophin, in contrast to dystrophin (18), could induce interfilament interaction, such as aggregation or bundling. This possibility was tested by measuring the effect of utrophin on the average fluorescence lifetime $\langle\tau\rangle$ (Eq. **8**) of 0.5 μM 5-((((2-iodoacetyl)amino)ethyl)amino)naphtalene-1-sulfonic acid (IAEDANS)-labeled filaments in the presence of 0.5 μM fluorescein-5-maleimide (Fmal)-labeled filaments. Whereas bundling of filaments was expected to decrease $\langle\tau\rangle$ because of fluorescence resonance energy transfer (FRET) between the neighboring IAEDANS- and Fmal-labeled filaments, $\langle\tau\rangle$ of IAEDANS actin before the addition of utrophin (11.3 $\pm$ 0.6 ns), was essentially the same as after the addition of 1 μM utrophin (11.5 $\pm$ 0.4 ns), indicating negligible (<2%) FRET. In contrast, bundling of filaments by the addition of 20 mM $MgCl_2$ (22) decreased $\langle\tau\rangle$ of IAEDANS-actin to 7.5 $\pm$ 0.8 ns, indicating $\approx$34% FRET

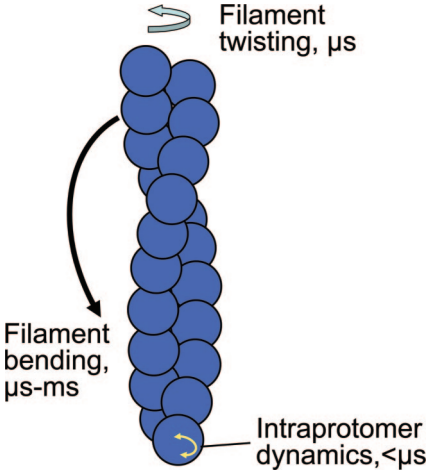

Fig. 4. Diagram of actin filament rotational dynamics.

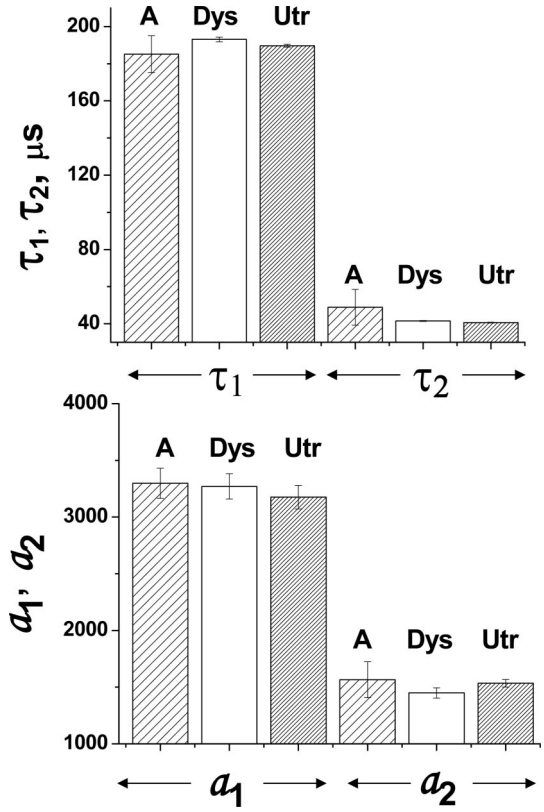

Fig. 5. Effect of dystrophin and utrophin on the lifetimes (τ) and amplitudes (a) of phosphorescence intensity decay of actin.

between the filaments. We conclude that utrophin does not induce bundling of actin filaments. This conclusion was confirmed by direct observation of phalloidin-rhodamine-labeled actin under a fluorescence microscope: complexes of 1 μM actin with 1 μM utrophin contained predominantly single filaments. Similar results were observed in complexes with 1 μM dystrophin. We conclude that the effects of utrophin and dystrophin on TPA of actin filaments (Figs. 2 and 3) reflect the internal dynamics of actin filaments, not interactions between filaments.

Discussion

Summary of Results. The binding of dystrophin or utrophin restricts the amplitudes of both submicrosecond and microsecond rotational dynamics of actin while increasing the microsecond rates (decreasing the correlation times). At a low level of actin saturation ($\leq$5%), both proteins induce similar changes in actin dynamics; but at higher levels, utrophin is more effective than dystrophin, causing greater restrictions in amplitude and increases in rates (Fig. 3).

Relationship to Models of Actin Rotational Dynamics. The actin rotational dynamics involves multiple modes and time scales (Fig. 4) (13): intraprotomer motions on the submicrosecond time scale, intrafilament torsional motions on the microsecond time scale, and filament bending motions on both microsecond and millisecond time scales (23). Our results indicate that utrophin affects all of these modes more profoundly than does dystrophin. One of these effects is restriction of the angular amplitudes of actin dynamics, on both the submicrosecond (Fig. 3*B*) and microsecond (Fig. 3 *A* and *D*) time scales, which is consistent with a previous electron microscopic study suggesting that a utrophin fragment restricts actin bending flexibility (11). However, our results also show that both proteins increase the rates of both bending and twisting motions, as evidenced by decreased correlation times in Fig. 3*C*. When analyzed by using the torsional twisting model (Eq. **5**), this indicates decreased torsional rigidity (increased torsional flexibility) by 26% for dystrophin and 78% for utrophin. These opposite effects on the amplitude and rate of actin microsecond dynamics have not been observed for other actin-binding proteins, which have been shown either to decrease [e.g., myosin or antibodies (16)] or to increase [e.g., gelsolin (14) or cofilin (15)] both amplitude and rate. These qualitatively unique effects of dystrophin and utrophin on actin dynamics are probably related to their physiological roles. These proteins do much more than stabilize actin filaments from depolymerization (9); they also manage to decrease the amplitude of actin bending and twisting flexibility while increasing the rates of these flexing motions. We suggest that these two effects serve to make actin stronger and more resilient, in analogy to the conversion of cast iron (strong but brittle) to steel (stronger and more resilient). It is likely that this results in greater resistance to filament breaking because of stretching (tensile strength) or twisting (torsional strength). This hypothesis suggests the importance of future direct single-filament mechanical measurements on the effects of these proteins on actin filaments.

All experiments in the present study were performed by using skeletal muscle α-actin. Although in vivo dystrophin and utrophin probably bind mainly to costameric γ-actin, it has been shown that the N-terminal actin-binding domain of dystrophin and intact dystrophin in the dystrophin–glycoprotein complex, bind α- and γ-actin with the same affinity (24). Binding of full-length utrophin is also essentially the same for muscle and nonmuscle actin isoforms (8). Thus, our results are relevant to interactions in vivo. Of course, future studies on the structural dynamics of γ actin will be illuminating.

Utrophin and Dystrophin Interact Differently with Actin. The different effects of dystrophin and utrophin on actin dynamics presumably result from distinct modes of contact between actin and these two proteins, as concluded from biochemical experiments (9). Detailed structural information about these contacts is currently limited to the actin-binding N-terminal domains of dystrophin and utrophin, Dys246 and Utr261. The analysis of electron micrographs of actin fully decorated with Dys246 and Utr261 showed that both of these proteins form extensive contacts with actin subdomains 1, 2, and 4 (11, 12), and qualitative differences observed between the structures of bound Dys264 and Utr261 suggest similarities and differences at the binding interfaces. One of the similarities is binding of the N-terminal parts of both proteins to the actin C terminus, as indicated by electron micrographs of the complexes (11) and proton NMR spectroscopy of peptides (25). Although this suggests that at least part of the observed effects of full-length dystrophin and utrophin on actin dynamics could result from direct effects of their N-terminal fragments on the probe-binding site at the C terminus, lack of substantial changes in the lifetime of the Cys-374-bound ErIA does not support this hypothesis. The large differences in the effects of the two proteins on actin dynamics must be understood in terms of their full-length structures: dystrophin has two separate low-affinity actin-binding sites whereas utrophin appears to bind via one contiguous actin-binding domain, so that the effects on actin dynamics detected via the ErIA probe probably reflect long-range cumulative effects from interaction at multiple binding sites. Our results suggest that the contiguous actin-binding domain of utrophin is more potent in perturbing actin rotational dynamics.

Implications for Pathophysiology. The effects of dystrophin and utrophin on actin structural dynamics could have profound physiological and pathological significance. We report two remarkable findings about the effects of these proteins on the actin-mediated linkage with the sarcolemma. First, dystrophin and utrophin both have a combination of effects not observed for actin-binding proteins: they restrict the amplitudes of actin microsecond flexibility while increasing the rates. These changes in actin flexibility may be important for optimal function of the actin–sarcolemma linkage, allowing for appropriate elastic response to muscle stretches, in both axial and torsional directions. Second, the two proteins have different effects on actin, both qualitatively and quantitatively, and these differences are more prominent at high actin saturation (Fig. 3). Because dystrophin and γ-actin are present in comparable concentrations in skeletal muscle, and these concentrations are well above K_d (9, 26), these differences between dystrophin and utrophin are physiologically relevant. The greater potency of utrophin in perturbing actin dynamics could make it an effective substitute even if expressed at lower levels than dystrophin in normal muscle. However, the different effects of utrophin at high levels suggest that the two proteins have different, as yet undetermined, functions in vivo. Future experiments using expressed fragments of dystrophin and utrophin and their functionally relevant mutants will determine which structural elements of these proteins are critical in determining the flexibility of actin filaments and what level of actin flexibility is physiologically optimal. The results of this research will provide insight into important functions of dystrophin and utrophin and will be informative to several therapeutic approaches for muscular dystrophies.

Methods

Preparation of Dystrophin and Utrophin. *Sf9* insect cells were infected with high-titer recombinant baculoviruses encoding FLAG-tagged full-length mouse dystrophin or utrophin (9) and incubated 72 h, and expressed protein was purified by anti-FLAG M2 affinity chromatography as described in ref. 8. The concentration of purified proteins was measured with the Bradford protein assay using BSA as a standard.

Preparation and Labeling of Actin. Actin was prepared from rabbit skeletal muscle as described in ref. 17, extracting acetone powder in cold water, polymerizing with 30 mM KCl for 1 h at room temperature, and centrifuging for 30 min at 300,000 $\times$ *g*. The pellet was suspended in G-Ca buffer [5 mM Tris

(pH 7.5), 0.5 mM ATP, 0.2 mM $CaCl_2$], clarified by 10 min centrifugation at 300,000 × *g*, and then polymerized with 2 mM $MgCl_2$ in 20 mM Tris (pH 7.5).

For phosphorescence experiments, actin was labeled at Cys-374 with ErIA (AnaSpec) as described in ref. 17. The dye, freshly dissolved in dimethylformamide, was added at a concentration of 480–48 μM F-actin. After a 2-h incubation at 25 °C, the labeling was stopped by 10 mM DTT, actin was ultracentrifuged for 30 min at 350,000 × *g*, pellets were suspended in Mg-G-buffer [5 mM Tris (pH 7.5), 0.2 mM $MgCl_2$, 0.5 mM ATP], clarified by 10-min centrifugation at 300,000 × *g*, and actin was polymerized (to F-actin) for 30 min at 25 °C by adding 2 mM $MgCl_2$. After ultracentrifugation for 30 min at 300,000 × *g*, pellets were suspended in UD buffer [100 mM NaCl, 2 mM $MgCl_2$, 10 mM Tris (pH 7.5), 0.2 mM ATP, 1 mM DTT], and the labeled F-actin (ErIA-actin) was immediately stabilized against depolymerization and denaturation by adding 1 molar equivalent of phalloidin. The extent of labeling, determined by measuring dye absorbance and protein concentration, was 0.99 ± 0.13 mol of dye per mol of actin, respectively. For fluorescence experiments, the same procedure was applied for labeling actin with IAEDANS and FMal. The extent of labeling with IAEDANS and FMal was 0.87 and 0.65 mol of dye per mol of actin, respectively. The concentration of unlabeled actin was measured by using a molar extinction coefficient of 0.63 mg of mL^{-1} cm^{-1} at 290 nm. The concentration of labeled actin was measured with the Bradford protein assay using unmodified actin as a standard; attached dyes had negligible effect on this assay.

Actin-Binding Analysis. Dystrophin and utrophin binding to actin filaments was measured by using high-speed cosedimentation (18). Varying concentrations of dystrophin and utrophin were added to 6 μM skeletal muscle F-actin, incubated for 30 min at 20 °C, and centrifuged at 100,000 × *g* for 20 min. The resulting pellets and supernatants were separated by SDS/PAGE and stained with Coomassie blue. The fractions of free and bound protein were quantified by densitometry. K_d and B_{max} of binding were obtained by fitting data by the function

$$y = B_{\max} * [P]/(K_d + [P]) \quad [1]$$

where y = bound protein (mol/mol actin) and [P] = free protein (μM).

Phosphorescence. For TPA experiments, phalloidin-stabilized ErIA-actin was diluted in UD buffer to 1.0 μM, and increasing concentrations of dystrophin or utrophin were added. To prevent photobleaching of the dye, oxygen was removed from the sample by 5-min incubation with glucose oxidase (55 μg/mL), catalase (36 μg/mL), and glucose (45 μg/mL) (17, 27). Phosphorescence was measured at 25 °C. Actin-bound ErIA was excited with a vertically polarized 1.2-ns pulse from a FDSS 532–150 laser (CryLas) at 532 nm, operating at a repetition rate of 100 Hz. Phosphorescence emission was selected by a 670-nm glass cutoff filter (Corion), detected by a photomultiplier (R928; Hamamatsu), and digitized by a transient digitizer (CompuScope 14100; GaGe) at a time resolution of 1 μs per channel. The time-resolved phosphorescence anisotropy decay was calculated as $r(t) = [I_v(t) - GI_h(t)]/[I_v(t) + 2GI_h(t)]$, where $I_v(t)$ and $I_h(t)$ are vertically and horizontally polarized components of the emission signal, detected at 90° with a single detector and a sheet polarizer that alternated between the two orientations every 500 laser pulses. G is an instrumental correction factor, determined by performing the measurement with horizontally polarized excitation, for which the corrected anisotropy value is set to zero. The time-dependent anisotropy decays of free actin and its complexes with dystrophin and utrophin were obtained by recording 30 cycles of 1,000 pulses (500 in each orientation of the polarizer).

TPA Data Analysis. The TPA decay was fitted with the function.

$$r(t) = r_1 \exp(-t/\phi_1) + r_2 \exp(-t/\phi_2) + r_\infty, \quad [2]$$

varying rotational correlation times, ϕ_1 (slow) and ϕ_2 (fast), the corresponding amplitudes, r_1 and r_2, and the final anisotropy r_∞. The initial anisotropy was then calculated as $r_0 = r(0) = r_1 + r_2 + r_\infty$. This method of analysis was established (16, 17) and was validated by comparing residuals and χ^2 for fits with one, two, and three exponential terms. These parameters were interpreted as follows: Increased initial anisotropy (r_0) indicates decreased amplitude of submicrosecond rotational dynamics, usually attributed to motion within the actin protomer. The angular amplitude of this submicrosecond motion, assuming a wobble in a cone with half-angle θ_c, is given by (13)

$$\theta_c(ns) = \cos^{-1}[-0.5 + 0.5(1 + 8\{r_0/0.205\}^{1/2})]. \quad [3]$$

Increased final anisotropy r_∞ (decreased r_1 and/or r_2) indicates decreased amplitudes of microsecond rotational dynamics (actin filament flexibility), and decreased correlation times (ϕ_1 and/or ϕ_2) indicate increased rates of microsecond rotation. The overall angular amplitude of microsecond motion, assuming a wobble in a cone, is given by (13)

$$\theta_c(\mu s) = \cos^{-1}[-0.5 + 0.5(1 + 8\{r_\infty/r_0\}^{1/2})]. \quad [4]$$

The separate amplitudes of the two modes of rotation can be estimated by substituting r_1 or r_2 for r_0 in Eq. **4**. In actin, the slower motion (ϕ_1, r_1) reflects primarily filament bending, whereas the faster motion (ϕ_2, r_2) reflects primarily filament twisting.

The torsional rigidity of actin was determined by fitting the TPA decay by a model assuming that actin is a continuous flexible rod (13):

$$r(t) = A_0 + A_1\exp[-0.25(t/\Phi)^{1/2}] + A_2\exp[-(t/\Phi)^{1/2}]. \quad [5]$$

The amplitudes A_i depend on orientation of the bound probe, and Φ is proportional to the torsional rigidity C of the filament, which is defined as the torque required to twist a 1-cm filament by 1 radian; for a completely rigid filament, $C = \infty$.

The phosphorescence lifetimes τ_i of actin-bound ErIA and their amplitudes a_i were obtained by fitting total phosphorescence intensity decay $I = [I_v(t) + 2GI_h(t)]/3$ by the function

$$I = a_1 \exp(-t/\tau_1) + a_2 \exp(-t/\tau_2). \quad [6]$$

Fluorescence Resonance Energy Transfer. Time-resolved fluorescence was measured with pulsed laser excitation and transient digitizer detection, as described in ref. 17. Actin-bound IAEDANS (donor) was excited with a 1 ns pulse from a passively Q-switched YAG laser (10-kHz repetition rate) at 355 nm. Time-dependent IAEDANS fluorescence emission $I(t)$ was detected at 465 nm, digitized (DS252; Aqiris), and analyzed by fitting to a sum of three exponentials terms plus a scattering component (Eq. **7**).

$$I(t) = \text{Scat} * \delta(0) + A_1\exp(-t/\tau_1) + A_2\exp(-t/\tau_2) + A_3\exp(-t/\tau_3). \quad [7]$$

Scat is the amplitude of scattered light, $\delta(0)$ is the δ function, A_i are amplitudes of fluorescence intensity decay, and τ_i are fluorescence lifetimes. The expression was convoluted with an excitation function $L(t)$ obtained from a light scattered from water. This convolution was then fit to the data by using an iterative nonlinear least-squares simulation with the Marquardt algorithm. The average lifetime $\langle\tau\rangle$ of donor (IAEDANS-labeled filaments) in the absence and presence of acceptor (FMal-labeled filaments) was determined as:

$$\langle\tau\rangle = (\Sigma A_i\,\tau_i)/\Sigma A_i, \qquad i = 1, 2, 3. \quad [8]$$

The efficiency of energy transfer E was calculated from the average lifetime of donor in the presence (τ_{DA}) and the absence (τ_D) of acceptor:

$$E = 1 - (\tau_{DA}/\tau_D). \quad [9]$$

Each result is reported as mean ± SEM ($n > 4$) unless indicated otherwise.

ACKNOWLEDGMENTS. We thank Octavian Cornea for assistance with preparation of the manuscript and Igor Negrashov for phosphorescence and fluorescence instrumentation and analysis software. This work was supported by Muscular Dystrophy Association Grant 4322 and National Institutes of Health Grants AR032961 and AG026160 (to D.D.T.) and by National Institutes of Health Grant AR042423 (to J.M.E.).

1. Straub V, Bittner RE, Leger JJ, Voit T (1992) Direct visualization of the dystrophin network on skeletal muscle fiber membrane. *J Cell Biol* 119:1183–1191.
2. Ervasti JM (2003) Costameres: The Achilles' heel of Herculean muscle. *J Biol Chem* 278:13591–13594.
3. Puttini, et al. (2008). Gene-mediated restoration of normal myofiber elasticity in dystrophic muscles. *Mol Ther* 17:19–25.
4. Petrof BJ, Shrager JB, Stedman HH, Kelly AM, Sweeney HL (1993) Dystrophin protects the sarcolemma from stresses developed during muscle contraction. *Proc Natl Acad Sci USA* 90:3710–3714.
5. Rybakova IN, Patel JR, Ervasti JM (2000) The dystrophin complex forms a mechanically strong link between the sarcolemma and costameric actin. *J Cell Biol* 150:1209–1214.

6. Winder SJ, et al. (1995) Utrophin actin-binding domain: Analysis of actin binding and cellular targeting. *J Cell Sci* 108:63–71.
7. Tinsley J, et al. (1998) Expression of full-length utrophin prevents muscular dystrophy in *mdx* mice. *Nat Med* 4:1441–1444.
8. Rybakova IN, Patel JR, Davies KE, Yurchenco PD, Ervasti JM (2002) Utrophin binds laterally along actin filaments and can couple costameric actin with sarcolemma when overexpressed in dystrophin-deficient muscle. *Mol Biol Cell* 13:1512–1521.
9. Rybakova IN, Humston JL, Sonnemann KJ, Ervasti JM (2006) Dystrophin and utrophin bind actin through distinct modes of contact. *J Biol Chem* 281:9996–10001.
10. Ervasti JM (2007) Dystrophin, its interactions with other proteins, and implications for muscular dystrophy. *Biochim Biophys Acta* 1772:108–117.
11. Galkin VE, et al. (2002) The utrophin actin-binding domain binds F-actin in two different modes: Implications for the spectrin superfamily of proteins. *J Cell Biol* 157:243–251.
12. Sutherland-Smith AJ, et al. (2003) An atomic model for actin binding by the CH domains and spectrin-repeat modules of utrophin and dystrophin. *J Mol Biol* 329:15–33.
13. Prochniewicz E, Zhang Q, Howard EC, Thomas DD (1996) Microsecond rotational dynamics of actin: Spectroscopic detection and theoretical simulation. *J Mol Biol* 255:446–457.
14. Prochniewicz E, Zhang Q, Janmey PA, Thomas DD (1996) Cooperativity in F-actin: Binding of gelsolin at the barbed end affects structure and dynamics of the whole filament. *J Mol Biol* 260:756–766.
15. Prochniewicz E, Janson N, Thomas DD, De la Cruz EM (2005) Cofilin increases the torsional flexibility and dynamics of actin filaments. *J Mol Biol* 353:990–1000.
16. Prochniewicz E, Thomas DD (1997) Perturbations of functional interactions with myosin induce long-range allosteric and cooperative structural changes in actin. *Biochemistry* 36:12845–12853.
17. Prochniewicz E, Walseth TF, Thomas DD (2004) Structural dynamics of actin during active interaction with myosin: Different effects of weakly and strongly bound myosin heads. *Biochemistry* 43:10642–10652.
18. Rybakova IN, Amann KJ, Ervasti JM (1996) A new model for the interaction of dystrophin with F-actin. *J Cell Biol* 135:661–672.
19. Prochniewicz E, Spakowicz DJ, Thomas DD (2008) Changes in actin structural transitions associated with oxidative inhibition of muscle contraction. *Biochemistry* 47:11811–11817.
20. Moores CA, Keep NH, Kendrick-Jones J (2000) Structure of the utrophin actin-binding domain bound to F-actin reveals binding by an induced fit mechanism. *J Mol Biol* 297:465–480.
21. Prochniewicz E, Thomas DD (1999) Differences in structural dynamics of muscle and yeast actin accompany differences in functional interactions with myosin. *Biochemistry* 38:14860–14867.
22. Strzelecka-Golaszewska H, Prochniewicz E, Drabikowski W (1978) Interaction of actin with divalent cations. 1. The effect of various cations on the physical state of actin. *Eur J Biochem* 88:219–227.
23. Thomas DD, Prochniewicz E, Roopnarine O (2002) Changes in actin and myosin structural dynamics due to their weak and strong interactions. *Results Probl Cell Differ* 36:7–19.
24. Renley BA, Rybakova IN, Amann KJ, Ervasti JM (1998) Dystrophin binding to nonmuscle actin. *Cell Motil Cytoskel* 41:264–270.
25. Levine BA, Moir AJ, Patchell VB, Perry SV (1992) Binding sites involved in the interaction of actin with the N-terminal region of dystrophin. *FEBS Lett* 298:44–48.
26. Hanft LM, Rybakova IN, Patel JR, Rafael-Fortney JA, Ervasti JM (2006) Cytoplasmic γ-actin contributes to a compensatory remodeling response in dystrophin-deficient muscle. *Proc Natl Acad Sci USA* 103:5385–5390.
27. Eads TM, Thomas DD, Austin RH (1984) Microsecond rotational motions of eosin-labeled myosin measured by time-resolved anisotropy of absorption and phosphorescence. *J Mol Biol* 179:55–81.